

Effects of 5%Ni addition on thermal stability and crystallization behavior of $\text{Mg}_{65}\text{Cu}_{25}\text{Tb}_{10}$ bulk metallic glass

QIN Wei-dong(秦卫东)¹, LI Jin-shan(李金山)¹, KOU Hong-chao(寇宏超)¹,

GU Xiao-feng(顾晓峰)², XUE Xiang-yi(薛祥义)¹, ZHOU Lian(周 廉)¹

1. State Key Laboratory of Solidification Processing, Northwestern Polytechnical University,
Xi'an 710072, China;

2. School of Information Technology and Engineering, Jiangnan University, Wuxi 214122, China

Received 22 August 2007; accepted 16 June 2008

Abstract: The effects of 5%Ni addition on the glass forming ability, thermal stability and crystallization behavior of $\text{Mg}_{65}\text{Cu}_{25}\text{Tb}_{10}$ bulk metallic glass were investigated using X-ray diffractometry, differential scanning calorimetry and transmission electron microscopy. The small amount of Ni addition reduces the glass forming ability and thermal stability due to a significant decrease in the crystallization activation energy. Analyses of crystallization kinetics give evidence to the existence of quenched-in nuclei in amorphous $\text{Mg}_{65}\text{Cu}_{20}\text{Ni}_5\text{Tb}_{10}$. Final crystallization products are basically same for $\text{Mg}_{65}\text{Cu}_{25}\text{Tb}_{10}$ and $\text{Mg}_{65}\text{Cu}_{20}\text{Ni}_5\text{Tb}_{10}$.

Key words: bulk metallic glass; thermal stability; crystallization behavior; quenched-in nuclei

1 Introduction

Since the discovery of Mg-Cu-Y bulk amorphous alloys in the early 1990s[1–2], Mg-based bulk metallic glasses(BMGs) have attracted wide attention due to their high specific strength, relatively low casting cost and excellent hydrogen storage capacities. The compositions were first extended to Mg-Cu-RE systems, where RE represents various rare-earth metals[3–6]. Then various transition metals, such as Ni and Ag, were selected to replace or partially replace Cu to improve the glass forming ability(GFA) and/or mechanical properties of these alloys[5–6]. Alloy addition is one of the simple and effective methods to improve the glass forming ability (GFA) and/or mechanical properties of amorphous metallic alloys. Recently, it is found that appropriate addition (5%) of Ni in $\text{Mg}_{65}\text{Cu}_{25}\text{Tb}_{10}$ significantly improves the mechanical properties[7]. Although some investigation has been made, the crystallization behavior needs to be further studied. In this work, we report the effects of 5%Ni addition on the glass-formability,

thermal stability and crystallization behaviors of amorphous Mg(CuNi)-Tb alloys.

2 Experimental

Cu-Tb and Cu-Ni-Tb master alloys were first prepared by arc melting Cu (99.99%, mass fraction), Ni (99.9%, mass fraction) and Tb (99.9%, mass fraction) under a Ti-gettered argon atmosphere in a water-cooled copper hearth. The ingot was then re-melted with pure Mg (99.99%) in an induction furnace under an argon atmosphere. Finally, cylindrical glassy samples of various sizes were prepared by the conventional copper mold casting method. The amorphous nature of the samples was examined by X-ray diffraction(XRD) (PHI-5400) using Cu K_{α} radiation. Thermal analyses were performed using differential scanning calorimetry (DSC) (Perkin-Elmer 2910) under a purified flowing argon. Different heating rates were applied to study the scanning rate dependence of the thermal parameters. Isothermal DSC scans were performed at appropriate temperatures in the undercooled liquid region to deter-

Foundation item: Projects(50601011, 50432020) supported by the National Natural Science Foundation of China; Project(A2720060295) supported by the Basic Research Project of National Defense of China; Project(BK2006533) supported by the Natural Science Foundation of Jiangsu Province, China; Project supported by the New Century Excellent Talents in University Program

Corresponding author: LI Jin-shan; Tel: +86-29-88491074; E-mail: ljsh@nwpu.edu.cn

mine the crystallization kinetics and to explore the mechanism of crystallization. Transmission electron microscopy(TEM) investigation was carried out by using a JEM-200EX (JEOL Tokyo, Japan) microscope operating at 200 kV.

3 Results and discussion

Fig.1 shows the XRD patterns taken from the cross-sectional surface of the as-cast $\text{Mg}_{65}\text{Cu}_{25-x}\text{Ni}_x\text{Tb}_{10}$ ($x=0, 5$) rods. The lack of sharp crystalline diffraction peaks, as well as the appearance of the broad strong scattering near 37° (2θ) indicates that the samples are essentially amorphous. The critical size with which the sample remains amorphous is represented by the largest amorphous diameter. It is found that D_c of $\text{Mg}_{65}\text{Cu}_{25-x}\text{Ni}_x\text{Tb}_{10}$ decreases gradually from 5 mm for the base alloy ($\text{Mg}_{65}\text{Cu}_{25}\text{Tb}_{10}$) to 4 mm for $\text{Mg}_{65}\text{Cu}_{20}\text{Ni}_5\text{Tb}_{10}$.

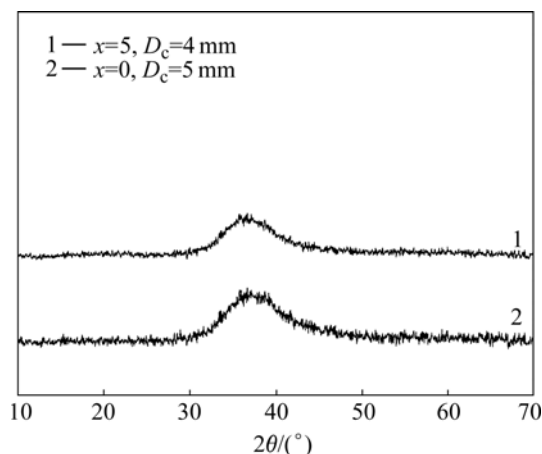


Fig.1 XRD patterns of as-cast $\text{Mg}_{65}\text{Cu}_{25}\text{Tb}_{10}$ (a) and $\text{Mg}_{65}\text{Cu}_{20}\text{Ni}_5\text{Tb}_{10}$ (b) bulk metallic glasses

Fig.2 presents the DSC curves of $\text{Mg}_{65}\text{Cu}_{25-x}\text{Ni}_x\text{Tb}_{10}$ ($x=0, 5$) at a constant heating rate of 40 K/min. Both curves exhibit an obvious endothermic event corresponding to the glass transition, as well as a large undercooled liquid region. The sharp exothermic peak corresponding to the major crystallization process is located at the peak temperature (T_p) of around 500 K. Characteristic temperatures such as T_g , T_x , T_p , T_m (solidus temperature) and T_l (liquidus temperature) are marked on the DSC curves. The accuracy of the determined temperatures is within ± 1 K. From Fig.2, we can find that T_g increases slightly from 424 K to 426 K, while T_x decreases from 488 K to 481 K due to the addition of 5% Ni. As a result, the width of the undercooled liquid region (defined as $\Delta T_x = T_x - T_g$) shrinks from 64 K to 55 K. The increase of T_g for the Ni-containing alloys is attributed to the enhancement of bonding forces among the constituent atoms[8]. A smaller ΔT_x usually implies a

weaker resistance to the nucleation and growth of crystalline phases, leading to a lower GFA[9]. Thus, the small amount of substitution Ni for Cu (e.g. 5%) deteriorates GFA and the thermal stability of $\text{Mg}_{65}\text{Cu}_{25}\text{Tb}_{10}$ amorphous alloys. If we compare the melting events of the above two compositions, we find that T_m of the $\text{Mg}_{65}\text{Cu}_{20}\text{Ni}_5\text{Tb}_{10}$ increases slightly with the addition of Ni, while T_l has a more significant increase, giving a larger melting range. As a result, the reduced glass transition temperature, T_{rg} (defined as $T_{rg} = T_g/T_l$) decreases from 0.570 for $\text{Mg}_{65}\text{Cu}_{25}\text{Tb}_{10}$ to 0.544 for $\text{Mg}_{65}\text{Cu}_{20}\text{Ni}_5\text{Tb}_{10}$. This tendency is consistent with the decrease of ΔT_x , which may suggest that the new composition is much away from the eutectic composition.

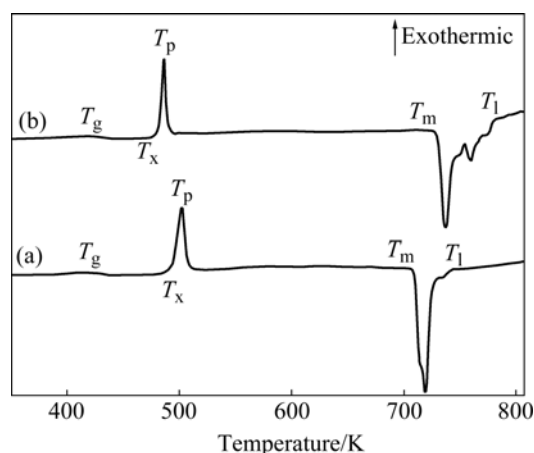


Fig.2 DSC curves of $\text{Mg}_{65}\text{Cu}_{25}\text{Tb}_{10}$ (a) and $\text{Mg}_{65}\text{Cu}_{20}\text{Ni}_5\text{Tb}_{10}$ (b) bulk metallic glasses at constant heating rate of 40 K/min

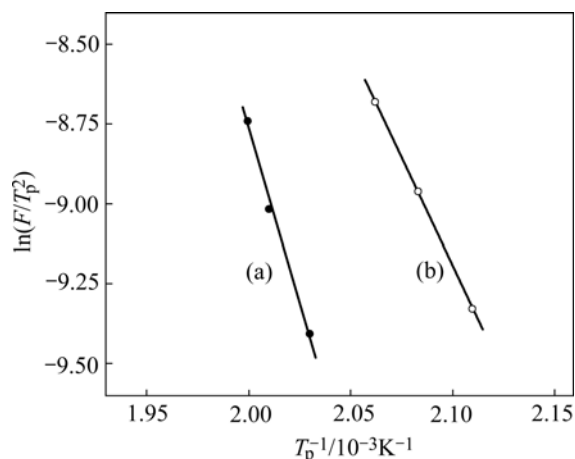
The heating rate dependence of characteristic temperatures was investigated (listed in Table 1). With increasing heating rate, the measured characteristic temperatures such as T_p increase slightly. This phenomenon is quite common for a kinetic process such as nucleation and growth[10], and was observed in similar bulk metallic glasses[11–13]. The relation between T_p and the heating rate can be analyzed by Kissinger's method to extract the activation energy[14]:

$$\ln \frac{F}{T_p^2} = -\frac{Q}{RT_p} + C_1 \quad (1)$$

where F is the heating rate, Q is the activation energy, R is the ideal gas constant and C_1 is an integration constant. Fig.3 shows plots of $\ln(F/T_p^2)$ as a function of $1/T_p$ for two different compositions. The activation energy is about 185 kJ/mol for the primary crystallization process of $\text{Mg}_{65}\text{Cu}_{25}\text{Tb}_{10}$. However, the activation energy is much lower for $\text{Mg}_{65}\text{Cu}_{20}\text{Ni}_5\text{Tb}_{10}$ (120 kJ/mol). This result indicates that the crystallization is easier to occur with 5% Ni addition, which is also consistent with the above analysis based on T_{rg} and ΔT_x .

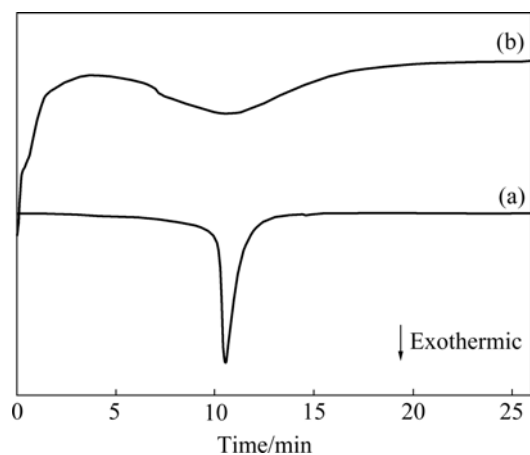
Table 1 Temperature dependence of characteristic temperatures of $\text{Mg}_{65}\text{Cu}_{25-x}\text{Ni}_x\text{Tb}_{10}$ ($x=0, 5$) bulk metallic glasses

Composition	Heating rate/($\text{K}\cdot\text{min}^{-1}$)	T_g/K	T_x/K	T_p/K	T_m/K	T_l/K	$\Delta T_x/\text{K}$	T_{rg}
$\text{Mg}_{65}\text{Cu}_{25}\text{Tb}_{10}$	20	416	475	493	705	737	59	0.564
	30	419	480	497	706	739	61	0.566
	40	424	488	500	707	742	64	0.570
$\text{Mg}_{65}\text{Cu}_{20}\text{Ni}_5\text{Tb}_{10}$	20	419	472	474	720	777	53	0.539
	30	421	475	480	722	778	54	0.541
	40	426	481	485	724	782	55	0.544

**Fig.3** Heating rate dependence of T_p for $\text{Mg}_{65}\text{Cu}_{25}\text{Tb}_{10}$ (a) and $\text{Mg}_{65}\text{Cu}_{20}\text{Ni}_5\text{Tb}_{10}$ (b) bulk metallic glasses

changing tendency.

Isothermal DSC scans were performed at 433 K in the undercooled liquid region to explore more information about the primary crystallization of $\text{Mg}_{65}\text{Cu}_{25-x}\text{Ni}_x\text{Tb}_{10}$ ($x=0, 5$), as shown in Fig.4. For $\text{Mg}_{65}\text{Cu}_{25}\text{Tb}_{10}$ (Fig.4(a)), the incubation time is about 7 min. The relatively long incubation time suggests that this composition is quite stable against nucleation. After 9 min of annealing, the crystallization starts and completes quickly. The rapid completion of crystalliza-

**Fig.4** Isothermal DSC curves of $\text{Mg}_{65}\text{Cu}_{25}\text{Tb}_{10}$ (a) and $\text{Mg}_{65}\text{Cu}_{20}\text{Ni}_5\text{Tb}_{10}$ (b) bulk metallic glasses (Annealing temperature 433 K)

tion (less than 4 min) suggests that the crystal growth rate is large in this case. However, $\text{Mg}_{65}\text{Cu}_{20}\text{Ni}_5\text{Tb}_{10}$ does not show an obvious incubation period before the onset of crystallization (Fig.4(b)), and the relatively sluggish crystallization process (larger than 10 min) corresponds to a lower crystal growth rate. This is attributed to the existence of quenched-in nuclei. Similar phenomena were observed in Mg-Cu-Ag-Y amorphous alloys[15].

The kinetics of such isothermal transformations can be analyzed using Johnson-Mehl-Avrami (JMA) equation[16]:

$$X(t)=1-\exp\{-k(t-\tau)^n\} \quad (2)$$

where $X(t)$ is the transformed volume fraction at time t , τ is the incubation time and n is the Avrami exponent. The combination of different growth mechanisms will produce different Avrami exponents[16].

The temperature dependence of the rate constant k can be described by the following Arrhenius equation:

$$k=k_0\exp(-Q/RT) \quad (3)$$

where k_0 is a constant, Q is the effective activation energy and R is the ideal gas constant. We can rewrite Eqn.(2) as

$$\ln[-\ln(1-X)]=\ln k+n\ln(t-\tau) \quad (4)$$

Then the Avrami exponent n can be obtained by fitting $\ln[-\ln(1-X)]$ vs $\ln(t-\tau)$ linearly, as shown in Fig.5. For $\text{Mg}_{65}\text{Cu}_{25}\text{Tb}_{10}$, n is about 2.3. This value is typical for crystallization governed by the diffusion-controlled growth of spherical grains, with the nucleation occurring at a decreased rate and low temperatures and increases to a constant rate at higher temperatures[12]. For $\text{Mg}_{65}\text{Cu}_{20}\text{Ni}_5\text{Tb}_{10}$, n is about 2.9. A typical Avrami exponent of 2.9 often implies that the crystallization starts from crystalline grains of small dimensions with an increased nucleation rate, namely, the linear growth of quenched-in nuclei[17]. All the above proofs suggest the existence of quenched-in nuclei in $\text{Mg}_{65}\text{Cu}_{20}\text{Ni}_5\text{Tb}_{10}$. However, the reason of forming those quenched-in nuclei after substituting only 5% Ni for Cu is still unknown.

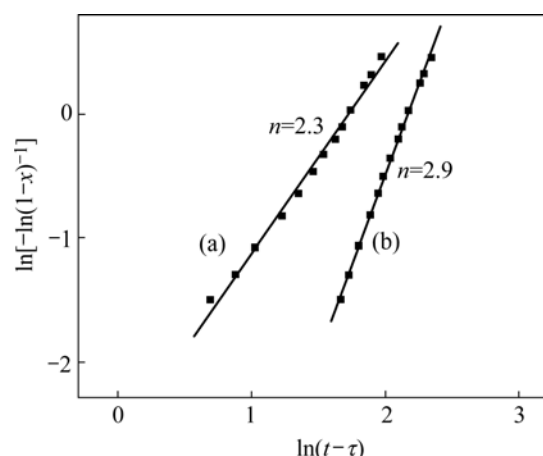


Fig.5 JMA plots of exotherm of $\text{Mg}_{65}\text{Cu}_{25}\text{Tb}_{10}$ (a) and $\text{Mg}_{65}\text{Cu}_{20}\text{Ni}_5\text{Tb}_{10}$ (b) bulk metallic glasses

Fig.6 shows TEM bright field(BF) images and selected area electron diffraction(SAED) patterns of the sample annealed at 433 K for 5 min. The BF image and the SAED pattern of $\text{Mg}_{65}\text{Cu}_{25}\text{Tb}_{10}$ in Fig.6(a) show that it is still amorphous after annealing, suggesting its high stability against crystal nucleation observed in the DSC

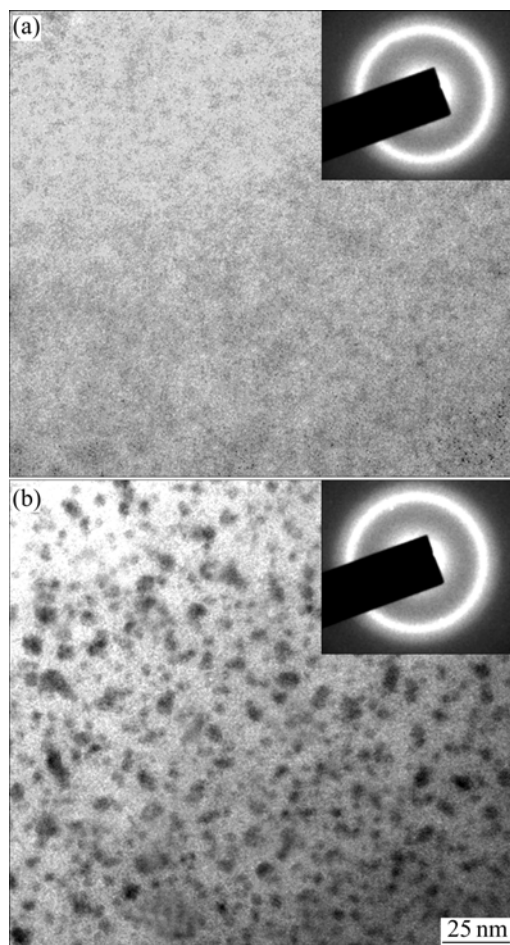


Fig.6 TEM bright-field images of $\text{Mg}_{65}\text{Cu}_{25}\text{Tb}_{10}$ (a) and $\text{Mg}_{65}\text{Cu}_{20}\text{Ni}_5\text{Tb}_{10}$ (b) annealed at 433 K for 5min

traces. However, very fine nanocrystalline particles can be observed in the samples for $x=5$ annealed for 5 min, consistent with the DSC observations. It is confirmed that quenched-in nuclei exists in the sample for $x=5$.

Finally, both the as-cast $\text{Mg}_{65}\text{Cu}_{25-x}\text{Ni}_x\text{Tb}_{10}$ ($x=0, 5$) bulk metallic glasses were annealed for 6 and 12 min at 510 K, a temperature just after the completion of the primary crystallization process. XRD examinations were performed on the annealed samples to identify the crystallization products and crystal growth rates (shown in Fig.7). For annealed $\text{Mg}_{65}\text{Cu}_{25}\text{Tb}_{10}$, the final crystallization products are α -Mg, Mg_2Cu , Mg_3Tb and some unknown phases. For annealed $\text{Mg}_{65}\text{Cu}_{20}\text{Ni}_5\text{Tb}_{10}$, the major crystalline phases are basically same as those of $\text{Mg}_{65}\text{Cu}_{25}\text{Tb}_{10}$. It seems that the small amount of Ni has not been involved in forming major phases.

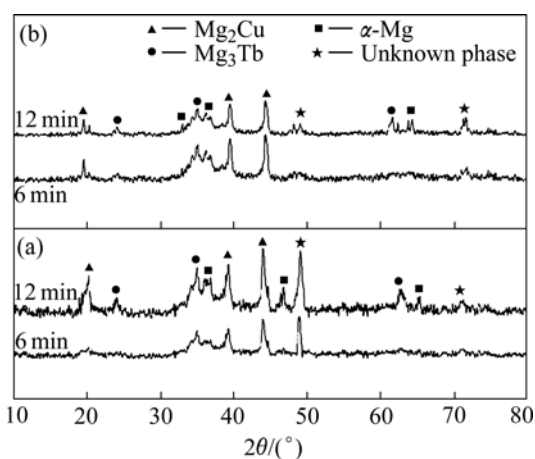


Fig.7 XRD patterns of $\text{Mg}_{65}\text{Cu}_{25}\text{Tb}_{10}$ (a) and $\text{Mg}_{65}\text{Cu}_{20}\text{Ni}_5\text{Tb}_{10}$ (b) bulk metallic glasses annealed at 510 K for different time

4 Conclusions

1) Although the small amount of Ni is helpful to increasing the glass transition temperature slightly, both the thermal stability and GFA deteriorate due to a remarkable reduction in the activation energy of crystallization.

2) Avrami analysis gives evidence to the existence of quenched-in nuclei in as-cast $\text{Mg}_{65}\text{Cu}_{20}\text{Ni}_5\text{Tb}_{10}$ glassy samples.

3) For annealed $\text{Mg}_{65}\text{Cu}_{20}\text{Ni}_5\text{Tb}_{10}$, the major crystalline phases are basically same as those of $\text{Mg}_{65}\text{Cu}_{25}\text{Tb}_{10}$. It seems that the small amount of Ni has not been involved in forming major phases.

References

- [1] GYOO K S, INOUE A, MASUMOTO T, High mechanical strengths of Mg-Ni-Y and Mg-Cu-Y amorphous alloys with significant supercooled liquid region [J]. Mater Trans JIM, 1990, 11: 929-934.
- [2] INOUE A, ZHANG T, KATO M T. Mg-Cu-Y bulk amorphous alloys with high tensile strength produced by a metallic mold casting

- method [J]. Mater Trans JIM, 1991, 32: 609–616.
- [3] ZHENG Q, CHENG S, STRADER J H, MA E, XUA J. Critical size and strength of the best bulk metallic glass former in the Mg-Cu-Gd ternary system [J]. Scripta Materialia, 2007, 56: 161–164.
- [4] XI X K, WANG R J, ZHAO D Q, PAN M X, WANG W H. Glass-forming Mg-Cu-RE (RE=Gd, Pr, Nd, Tb, Y, and Dy) alloys with strong oxygen resistance in manufacturability [J]. Journal of Non-Crystalline Solids, 2004, 344: 105–109.
- [5] MA H, ZHENG Q, XU J, LI Y, MA E. Doubling the critical size for bulk metallic glass formation in the Mg-Cu-Y ternary system [J]. Materials Research, 2005, 20(9): 2252–2255.
- [6] XI X K, ZHAO D Q, PAN M X. Highly processable Mg₆₅Cu₂₅Tb₁₀ bulk metallic glass [J]. Journal of Non-Crystalline Solids, 2004, 344: 189–192.
- [7] ZHANG Qing-rong, LI Jin-shan, WANG Yi-chuan, KOU Hong-cai, HU Rui, ZHOU Lian, FU Heng-zhi. Effect of substitution of Ni for Cu on glass forming ability and mechanical properties of Mg-Cu-Tb metallic glass alloys [J]. The Chinese Journal of Nonferrous Metals, 2007, 17(2): 303–307. (in Chinese)
- [8] FANG Shou-shi, XIAO Xue-shan, XIA Lei, LI Wei-huo, DONG Yuan-da. Relationship between the widths of supercooled liquid regions and bond parameters of Mg-based bulk metallic glasses [J]. Journal of Non-Crystalline Solids, 2003, 321: 120–125.
- [9] YUAN G Y, INOUE A. The effect of Ni substitution on the glass-forming ability and mechanical properties of Mg-Cu-Gd metallic glass alloys [J]. Journal of Alloys and Compounds, 2005, 387: 134–138.
- [10] LU Z P, LIU C T. Glass formation criterion for various glass-forming systems [J]. Phys Rev Lett, 2003, 91: 115505–11508.
- [11] MURTY B S, HONO K. Forming of nanocrystalline particle in glassy matrix in melt-spun Mg-Cu-Y based alloys [J]. Mater Trans JIM, 2000, 41: 1538–1544.
- [12] HE Lin, SUN Jun, LI Yang. Effect of Sc on crystallization kinetics of Zr-based bulk amorphous alloy [J]. The Chinese Journal of Nonferrous Metals, 2006: 16(1): 35–40. (in Chinese)
- [13] MEN H, KIM W T, KIM D H. Glass formation and crystallization behavior in Mg₆₅Cu₂₅Y_{10-x}Gd_x (x=0, 5 and 10) alloys [J]. Journal of Non-Crystalline Solids, 2004, 337: 29–35.
- [14] KISSINGER H E. Variation of peak temperature with heating rate in differential thermal analysis [J]. Anal Chem, 1957, 29: 1702–1706.
- [15] MADGE S V, GREER A L. Effect of Ag addition on the glass-forming ability and thermal stability of Mg-Cu-Y alloys [J]. Mater Sci Eng A, 2004, 375: 759–762.
- [16] AVRAMI M. Granulation phase change and microstructure [J]. J Chem Phys 1941, 9: 177–184.
- [17] CHRISTIAN J W. The theory of transformations in metals and alloys (Parts I and II) [M]. Oxford, UK: Pergamon Press, 2002: 544–547.

(Edited by YANG Bing)